Catal Lett (2009) 128:434–442
DOI 10.1007/s10562-008-9770-4

# Selective Oxidation of Benzyl Alcohol Over Copper Phthalocyanine Immobilized on MCM-41

**A. Hamza · D. Srinivas**

Received: 18 September 2008 / Accepted: 6 November 2008 / Published online: 22 November 2008
© Springer Science+Business Media, LLC 2008

**Abstract** Copper phthalocyanine (CuPc) complexes immobilized on "neat" and $Ti^{4+}$ and $Al^{3+}$ containing MCM-41 mimic the functionality of metalloenzymes. These novel materials catalyze the oxidation of benzyl alcohol to selectively benzaldehyde at moderate temperatures using peroxides and molecular oxygen as oxidant. Electron paramagnetic resonance and X-ray photoelectron spectroscopic studies revealed that the acidity of the support (MCM-41) influences the electronic structure of the immobilized CuPc. On acidic supports a part of copper in CuPc got reduced from a "formal" +2 to +1 oxidation state. This reduction of copper in its oxidation state on different supports decreased in the order: Al-MCM-41 (Brönsted and strong Lewis acid sites) > MCM-41 (silanol sites) > Ti-MCM-41 (weak Lewis acid sites). A linear variation in catalytic activity with the concentration of $Cu^{1+}$ ions in different catalyst samples was observed. The study reveals that by suitably modifying the acidic properties of the support one can, in principle, fine-tune the electronic and catalytic properties of the active oxidation sites.

**Keywords** Selective oxidation of benzyl alcohol · Copper phthalocyanine · MCM-41 · EPR · UV–visible spectroscopy

A. Hamza · D. Srinivas (✉)
Catalysis Division, National Chemical Laboratory, Pune 411 008, India
e-mail: d.srinivas@ncl.res.in

## 1 Introduction

One of the major challenges in catalysis research is to design and develop selective oxidation catalysts that operate at mild conditions [1]. Oxidation of benzyl alcohol to benzaldehyde (without forming further oxidation products like benzoic acid) is an important organic transformation. This reaction is widely investigated as it provides chlorine-free benzaldehyde required in perfumery and pharmaceutical industries [2, 3]. Traditionally, this transformation is carried out using stoichiometric amounts of chromium and manganese reagents [4–6]. These oxidants are not only expensive but generate copious amounts of toxic heavy-metal waste. Moreover, the reaction is often performed in environmentally undesirable solvents like chlorinated hydrocarbons. Selective liquid phase oxidation with peroxides or molecular oxygen is a greener approach. Supported, nanoscopic noble metal catalysts (Pt, Pd, Au, and their alloys) have been investigated for this reaction under solvent-free conditions [7–14]. However, over oxidation and catalyst deactivation are some of the issues with those catalysts. Several metal oxide-based catalysts have also been reported. With most of those catalysts the selectivity for benzaldehyde is lower than that obtained in the commercial manufacturing process [15–19]. Hence, in view of the atom-economy, development of an efficient and selective oxidation catalyst that operates at mild reaction conditions and utilizes peroxides or molecular oxygen as oxidant is highly desirable. The present study reports oxidation of benzyl alcohol over Copper phthalocyanine (CuPc) immobilized on MCM-41 and Ti- and Al-containing MCM-41. It may be noted that, in nature, this oxidation reaction is catalyzed at ambient conditions by galactose oxidase, a monomeric, Type-II, copper enzyme [20, 21].

CuPc was chosen as it is known to mimic the functionality of metalloenzymes [22]. Metal complexes when encapsulated inside the supercages of zeolites, their catalytic activity and selectivity were enhanced [23–25]. The superior performance of these zeozymes (*acronym* for zeolite mimics of enzymes) was attributed to molecular conferment effects and support-metal complex interactions. In this study, for the first time, we have delineated the effect of the latter from that of the former type interaction on the structure and catalytic properties of CuPc. The effect of confinement is less important in mesoporous M41S-type materials than in microporous zeolites. The acidity of the support is varied by incorporating $Ti^{4+}$ (which generate weak Lewis acid sites) and $Al^{3+}$ (which generate strong Lewis and Brönsted acid sites) in the framework of MCM-41. Further, the density of the acid sites was varied by changing the Si/metal ratio. The support materials were prepared by the known hydrothermal methods. CuPc (2–4 wt%) was immobilized on MCM-41, Ti-MCM-41 ($SiO_2/TiO_2 = 20$ and 40), and Al-MCM-41 ($SiO_2/Al_2O_3 =$ 10–50) by impregnation technique. The materials were characterized by several physicochemical techniques. A comparative spectroscopic and catalytic activity study reveals that there exists a correlation between acidity of the support and catalytic activity of immobilized CuPc complexes.

## 2 Experimental

### 2.1 Catalyst Preparation

#### *2.1.1 "Neat" MCM-41, Al-MCM-41, and Ti-MCM-41*

Siliceous MCM-41 was prepared according to the known procedure [26] using sodium silicate (Aldrich Co) as the source of silicon and cetyltrimethylammonium bromide (CTABr; S. D. Fine Chem. Ltd, India) as the surfactant. The composition of the synthesis gel was—$SiO_2$:0.31CTABr:35.5$H_2O$. In a typical preparation, 8.67 g of CTABr was dissolved in 29 g of distilled water while stirring. To it, 9.35 g of sodium silicate was added drop-wise for 20 min. Stirring was continued for 1 h and then, 0.609 g of conc. $H_2SO_4$ in 2.5 ml of distilled water was added drop-wise. The mixture was stirred further at 298 K for 1–2 h. The gel was transferred to a Teflon-lined stainless steel autoclave and aged for 24 h at 373 K. The slurry was filtered and washed thoroughly with distilled water. It was dried at 373 K and calcined at 823 K for 6 h to remove the occluded template molecules.

Al-MCM-41 was prepared in the same manner except that a required quantity of sodium aluminate (source of Al; Aldrich Co) dissolved in 20 mL of distilled water was added drop-wise after the addition of sodium silicate in the above procedure [26, 27]. The composition of the synthesis gel of Al-MCM-41 was—$SiO_2$:0.31CTABr:35.5$H_2O$:*x*-$Al_2O_3$, where *x* varies from 0.1 to 0.02 to produce mesoporous silica materials with $SiO_2/Al_2O_3$ molar ratio of 10–50.

Ti-MCM-41 was synthesized [28] using the gel composition—$SiO_2$:*x*Ti-isopropoxide:0.245CTABr:0.487 NaOH:19.4$H_2O$, where *x* varies from 0.08 to 0.01 to produce mesoporous titanosilicates with $SiO_2/TiO_2$ molar ratio of 12.5 to 100. In a typical preparation of Ti-MCM-41 ($SiO_2/TiO_2 = 30$), 1.305 g of NaOH was dissolved in 144 g of distilled water. CTABr (5.943 g) was added while stirring. Then, 4 g of fumed silica (source of Si; Aldrich Co) was added in 1–1.5 h with constant stirring. This slurry was stirred for 1–2 h. The pH of the slurry was adjusted to 9–10 using dilute $H_2SO_4$. Ti-isopropoxide (source of Ti; 0.657 g; Aldrich Co) dissolved in iso-propanol was added to the above in 15–20 min. It was kept for stirring for another 5–6 h and aged at 373 K for 48 h in a Teflon-lined autoclave. The resulting solid was filtered, washed thoroughly with distilled water and dried at 373 K for 1 h. The as-synthesized Ti-MCM-41, thus prepared, was calcined for 6 h at 723 K.

#### *2.1.2 MCM-41—Immobilized CuPc Complexes*

CuPc (Aldrich Co, 0.085 g) was dissolved in 80 mL of dry-toluene. It was then added slowly to a suspension of 2 g of mesoporous silica (MCM-41, Al-MCM-41 or Ti-MCM-41) in toluene. The reaction mixture was refluxed for 15 h. The blue solid formed was separated by filtration. It was Soxhlet extracted with a series of solvents in the order acetone, toluene, pyridine and acetone for several hours to remove any loosely bound CuPc molecules. Later, the solid silica-encapsulated CuPc was filtered and dried at 405 K for 2 h to remove the adsorbed solvent molecules. Varying amounts of CuPc immobilized on "neat" and Al- and Ti-containing MCM-41 were prepared. The catalyst samples were designated as Me-MCM-41(*x*)-CuPc(*y*), where Me refers to Si, Al or Ti, *x* to molar ratio of $SiO_2/TiO_2$ or $SiO_2/Al_2O_3$, and *y* to weight percent of immobilized CuPc.

### 2.2 Catalyst Characterization

The chemical composition of the catalysts was determined using energy dispersive X-ray (EDX; FEI-USA, Quanta 2003D) and C, H, and N-elemental analyses (Carlo Erba; EA1108) techniques. Low-angle X-ray powder diffraction (XRD) patterns were recorded on an X'Pert Pro Philips diffractometer equipped with Cu-$K_\alpha$ radiation and a proportional counter detector. Textural properties were determined from nitrogen physisorption measurements

conducted on a Coulter Omnisorb 100 CX instrument. Thermal analysis of the samples was done on a Perkin–Elmer Diamond TG-DTA instrument. Diffuse reflectance UV–visible (DRUV-vis) spectra of the catalysts were recorded on a Shimadzu (UV-2500 PC) spectrophotometer using spectral grade $BaSO_4$ as the reference material. Fourier transform infrared (FTIR) spectra of the samples (as KBr pellets) were recorded on a Shimadzu 8201 PC spectrophotometer in the region 400–4,000 $cm^{-1}$. Electron paramagnetic resonance (EPR) spectra were recorded on a Bruker EMX X-band spectrometer at 298 K. X-ray photoelectron spectroscopy (XPS) measurements were conducted on a VG Microtech Multilab ESCA 3000 spectrometer with Mg-$K_\alpha$ radiation ($hv = 1{,}253.6$ eV). Diffuse reflectance Fourier transform infrared spectra of pyridine adsorbed on selected MCM-41 samples were recorded on a Shimadzu SSU 8000 (DRIFT IR) spectrometer equipped with a liquid nitrogen-cooled MCT detector. Samples were activated at 473 K for 2 h under nitrogen flow. Then, they were cooled to 323 K and pyridine (30 μL) was adsorbed. The sample temperature was raised to a desired value (323–473 K) and held at that temperature for 30 min and then, the spectrum was recorded.

### 2.3 Reaction Procedure

The oxidation of benzyl alcohol was carried out in liquid-phase at atmospheric pressure and in the presence of immobilized CuPc complexes. In a typical experiment, 5 mmol of benzyl alcohol and 10 mL of solvent were taken in a glass round bottomed flask, placed in a constant temperature oil bath. To it, 0.055 g of the catalyst and 7.5 mmol of oxidant (tert.-butyl hydroperoxide; 70% aq. solution) were added. The reaction was conducted while stirring at 373 K for 4 h. The catalyst was separated by filtration and the filtrate was analyzed by gas chromatography (Varian 3400; CP-SIL8CB column; 30 m-long and 0.53 mm-i.d.). The products were identified by GC-MS (Varian CP-3800; CP-SIL8CB capillary column; 30 m-long, 0.25 mm-i.d., and 0.25 μm thick) using standard samples. In certain studies, the reactions were conducted using molecular oxygen (1 atm) instead of tert.-butyl hydroperoxide.

## 3 Results and Discussion

### 3.1 Structure and Spectroscopic Characterization

The MCM-41 samples showed well-resolved, low-angle XRD peaks (Fig. 1) confirming the mesoporous architecture and long-range ordering [29, 30]. Incorporation of $Ti^{4+}$ and $Al^{3+}$ ions in the framework of MCM-41 shifted the XRD peaks to higher $2\theta$ values. The extent of such a shift increased with increasing metal content. Also a decrease in intensity and broadening of (100) peak was noted with increasing metal content in MCM-41. These variations in diffraction patterns are a clear indication of modification in the texture of these materials due to hetero-atom substitution. Similar observations were found also in our earlier studies [29, 30]. The variation in XRD peaks position indicated that up to a metal loading of $SiO_2/TiO_2 = 30$, $Ti^{4+}$ ions go into the silica lattice and above that they occupy the surface as extra lattice titanium. In the case of Al-MCM-41, Al could be incorporated up to a molar ratio of $SiO_2/Al_2O_3 = 20$. The broadening of XRD peak at higher metal ion loading indicates a relatively wider distribution of pore sizes in Ti and Al containing MCM-41. The long-range mesoporous ordering of MCM-41 is retained even after the metal complex immobilization (Fig. 1). The d-spacing and unit cell parameters (estimated from the positions of the XRD peaks) agree well with those reported by others (Table 1) [26–28].

All the materials showed typical type-IV, $N_2$ adsorption/desorption isotherms ($S_{BET} = 670$–$963$ $m^2/g$; pore diameter = 3.0–3.9 nm; total pore volume = 0.77–0.98 cc/g).

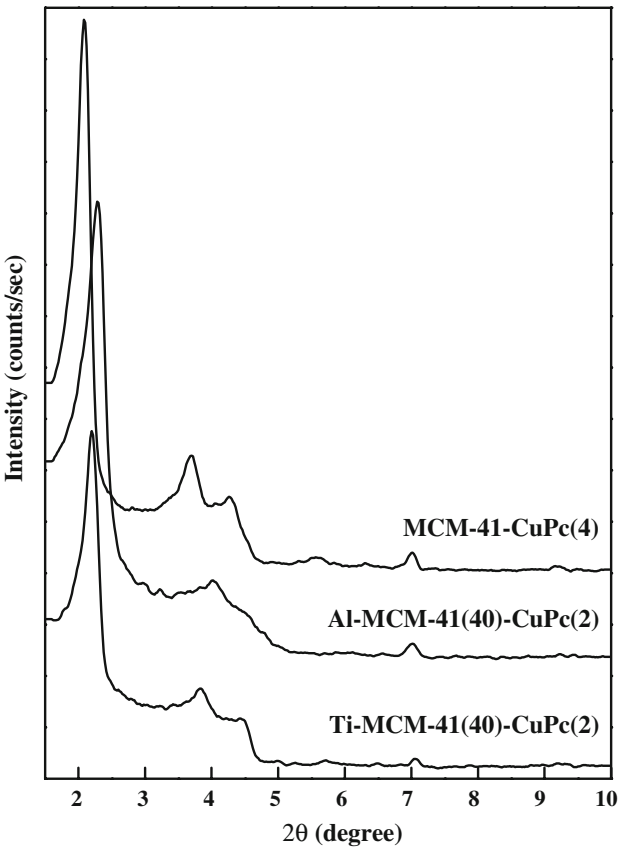


**Fig. 1** X-ray diffractograms of MCM-41-immobilized CuPc

**Table 1** Chemical composition, XRD and thermal analysis of CuPc immobilized on MCM-41

| Material | Elemental analysis | | | XRD | | Thermal analysis: % weight loss | | | |
|---|---|---|---|---|---|---|---|---|---|
| | C (wt%) | N (wt%) | C/N ratio | $d_{100}$ (nm) | Unit cell parameter (nm) | Stage-I (308–378 K) | Stage-II (378–678 K) | Stage-III (678–798 K) | Stage-IV (798–1,073 K) |
| MCM-41-CuPc(4) | 2.6 | 1.1 | 2.3 | 4.2 | 4.9 | 6.9 | 3.4 | 4.0 | 3.1 |
| Ti-MCM-41(20)-CuPc(4) | 2.9 | 1.1 | 2.6 | 3.8 (3.8) | 4.4 (4.3) | 6.0 | 3.7 | 4.4 | 3.1 |
| Ti-MCM-41(40)-CuPc(2) | 1.7 | 0.7 | 2.5 | 4.0 (4.0) | 4.6 (4.6) | 5.7 | 4.3 | 3.2 | 2.3 |
| Ti-MCM-41(40)-CuPc(4) | 3.3 | 1.1 | 3.1 | 3.8 (4.0) | 4.4 (4.6) | 4.3 | 3.0 | 4.5 | 3.2 |
| Al-MCM-41(10)-CuPc(4) | 3.0 | 1.1 | 2.9 | 4.0 (3.9) | 4.6 (4.5) | 7.2 | 4.9 | 4.3 | 3.3 |
| Al-MCM-41(20)-CuPc(4) | 2.4 | 0.8 | 3.2 | 4.1 (4.0) | 4.8 (4.6) | 5.2 | 4.7 | 4.7 | 3.1 |
| Al-MCM-41(40)-CuPc(2) | 2.0 | 0.7 | 2.7 | 3.8 (4.1) | 4.4 (4.7) | – | – | – | – |
| Al-MCM-41(40)-CuPc(4) | 3.2 | 1.3 | 2.6 | 4.1 (4.1) | 4.7 (4.7) | 6.4 | 4.0 | 5.0 | 2.1 |
| Al-MCM-41(50)-CuPc(4) | – | – | – | 4.1 (4.0) | 4.7 (4.6) | 7.5 | 5.5 | 6.7 | 3.0 |

The presence of Cu in the catalyst samples was confirmed by EDX. The carbon/nitrogen ratio for "neat" CuPc is 3.3. This value for immobilized complexes (estimated from elemental analysis) is in close agreement with that of the "neat" CuPc (Table 1) indicating that the metal complex is indeed immobilized on the mesoporous silica materials. Scanning electron micrographs revealed a rectangular morphology for these materials.

Thermogravimetric analysis (TGA) showed two stages (I and III) of exothermic weight loss in a relatively narrow temperature range and two more stages (II and IV) in broader temperature range (Table 1): Stages I (308–378 K; 5–7%) and II (378–678 K; 3–5.5%) correspond to loss of occluded water from the meso and micropores of MCM-41, respectively. Stage III (678–798 K; 4–5%) is due to decomposition of phthalocyanine moiety as well as condensation of some silanol groups ($2SiOH \rightarrow Si–O–Si + H_2O$). Stage IV (798–1,073 K; 3%) is due to condensation of silanol groups only. It may be noted that the losses due to condensation of silanol groups were ascertained by doing independent experiment on "neat" Ti/Al-MCM-41. Subtraction of weight loss due to silanol condensation enabled an estimation of about 1.7% loading of CuPc in Ti/Al-MCM-41(40)-CuPc(4).

The acidic properties of the samples were determined by DRIFT spectroscopy of adsorbed pyridine. The spectra of pyridine adsorbed on Ti-MCM-41 revealed the absence of Brönsted (1,546 and 1,639 $cm^{-1}$) and strong Lewis (1,623 and 1,455 $cm^{-1}$) acid sites. Only weak Lewis acid sites (1,577 and 1,488 $cm^{-1}$) and H-bonded pyridine sites (1,595 and 1,444 $cm^{-1}$) were present [28]. "Bare" MCM-41 showed IR peaks typical of H-bonded pyridine. Al-MCM-41(40) contained Brönsted as well as strong Lewis acid sites. The DRIFT spectra revealed that Ti incorporation generated only the weak Lewis acid sites and Al incorporation, on the other hand, generated both Brönsted and Lewis acid sites.

FTIR spectra (Fig. 2) showed a sharp peak at 950 $cm^{-1}$, in case of Ti/Al-MCM-41, confirming the incorporation of heteroatom (Ti/Al) in the framework of mesoporous silica. The characteristic peaks due CuPc are, in general, masked by the intense silica framework peaks due to smaller concentration of the former (Fig. 2).

"Neat" CuPc showed an UV–vis spectrum with a Soret band at 431 nm and four Q-bands at 553, 593, 678, and 759 nm. In the case of a perfect square planar geometry for Pc, one should observe only two Q-bands. However, occurrence of four instead of two Q-bands indicates that CuPc is non-planar. Similar observations were found by us earlier when CuPc was encapsulated inside the pores of zeolite-Y [25]. Upon immobilization on MCM-41, a marked shift in the position of these bands was observed (Fig. 3). While the Soret band had undergone a blue shift to 429 nm, the Q-bands exhibited a red shift to 567, 685, and 745 nm. The shift in band position and changes in relative intensity of these bands indicate high dispersion and variation in the geometry of Pc molecules. The red shift in Q-bands increased in different immobilized complexes in the order: MCM-41-CuPc < Ti-MCM-41-CuPc < Al-MCM-41-CuPc. In other words, the acidity of the support plays a crucial role. The support-metal complex interaction increased with the acidity. The acidic moieties of the support (silanol in case of MCM-41, Lewis acid Ti in Ti-MCM-41 and Brönsted acid and Lewis acid Al in Al-MCM-41) possibly interact with the electron rich nitrogen atoms of the ring and enable stronger support-metal complex interactions. Since the acidity of Al-MCM-41 is higher and the interaction is stronger, a significant amount of electron transfer from CuPc to the support would have taken place, and as a consequence, the

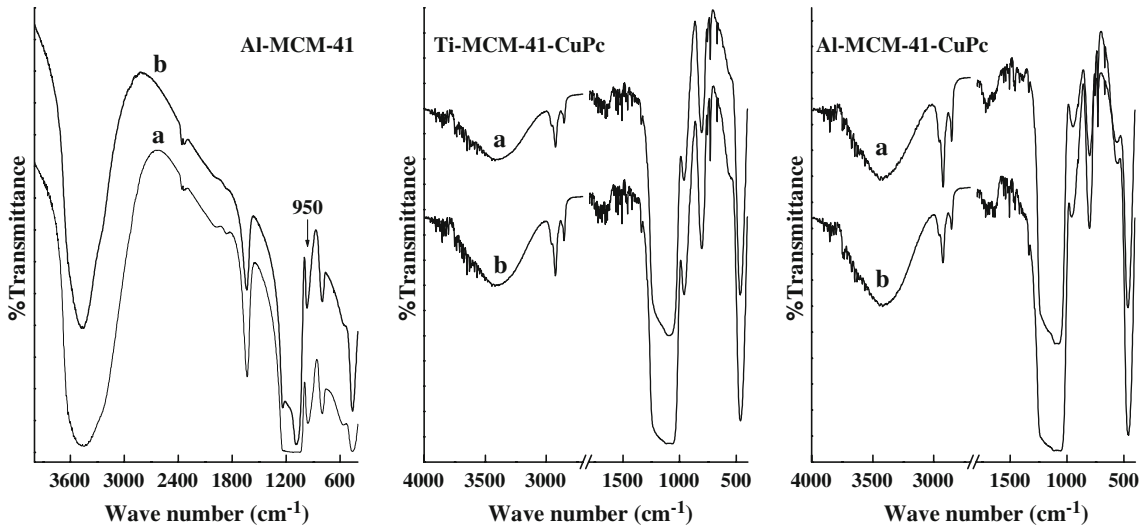


**Fig. 2** FTIR spectra: *Left* Al-MCM-41–$SiO_2/Al_2O_3 = 10$ (*a*) and 40 (*b*). *Middle* Ti-MCM-41-CuPc (4%)–$SiO_2/TiO_2 = 20$ (*a*) and 40 (*b*). *Right* Al-MCM-41-CuPc (4%)–$SiO_2/Al_2O_3 = 10$ (*a*) and 40 (*b*)

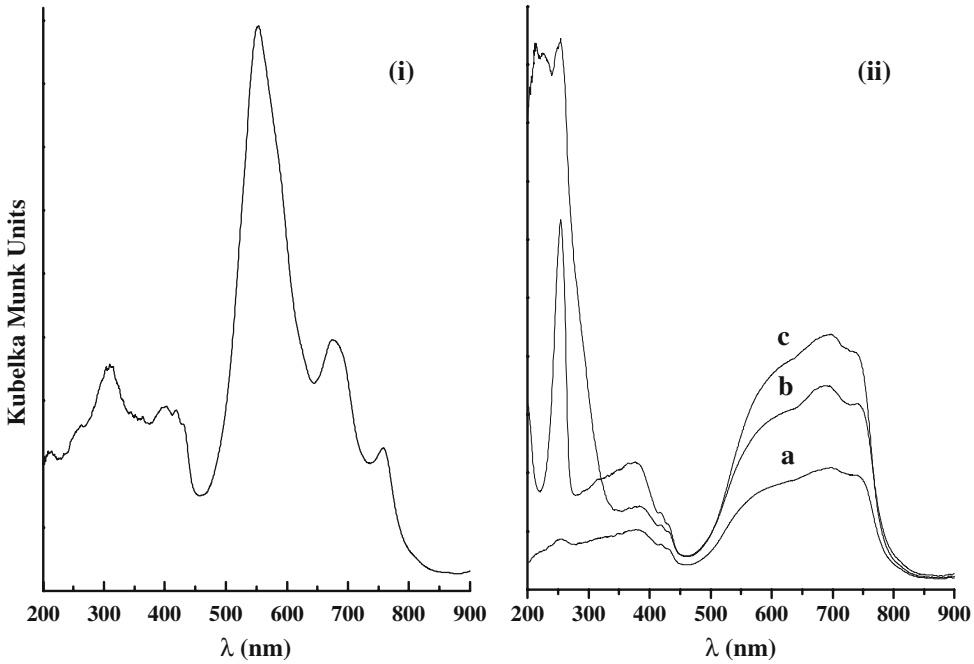


**Fig. 3** DRUV-vis spectra: (i) "neat" CuPc and (ii) immobilized CuPc—(*a*) MCM-41-CuPc(4), (*b*) Ti-MCM-41(40)-CuPc(4) and (*c*) Al-MCM-41(40)-CuPc(4)

electronic structure of CuPc supported on strongly acidic sites had significantly altered.

Fig. 3(ii) shows that the amount of CuPc immobilized on different supports increases in the order: MCM-41 < Ti-MCM-41 < Al-MCM-41. The amount of CuPc immobilized increased with an increase in Al content in Al-MCM-41 up to $SiO_2/Al_2O_3 = 40$ and thereafter it had decreased. It is known that Al or Ti can be incorporated up to some amount in the framework of MCM-41 and above that it is present as extra-framework oxide on the surface of MCM-41. Presence of extraframework metal oxide is detrimental for immobilization of CuPc.

"Neat" CuPc showed an EPR spectrum with $g\| = 2.15$ and $g_\perp = 2.04$ [25]. The hyperfine features due to copper could not be resolved due to intermolecular interactions. The immobilized complexes showed a relatively narrow, asymmetric signal with partially resolved parallel features (Fig. 4). The narrow signal is an indication of lowered intermolecular interactions and dispersion/isolation of CuPc molecules. The normalized EPR signal intensity was lower for the complexes immobilized on Al-MCM-41 than on Ti-MCM-41 (Fig. 4(i)). If we recall the DRUV-vis data, the amount of CuPc immobilized was, in fact, higher on the former than on the latter support (Fig. 3(ii); note the

difference in the intensities of Q-bands). Also the interaction was found to be more on Al than on Ti-MCM-41 supports (UV–vis). Because of stronger interaction, more amount of electron density is delocalized from Cu to the support and thereby the metal ions are partially reduced. As a consequence, the EPR signal intensity is lower for CuPc immobilized on Al- than on Ti-MCM-41 supports. EPR spectroscopy also revealed that the amount of CuPc immobilized increased with increasing Al content up to $SiO_2/Al_2O_3 = 40$ and thereafter it decreased. It also revealed that the amount of CuPc immobilized increased with increasing concentration of CuPc in the impregnation process (Fig. 4(ii)). All these observations reconfirm the conclusions drawn from DRUV-vis spectroscopy.

To substantiate the EPR results, XPS of CuPc supported on Al-MCM-41 and Ti-MCM-41 were recorded. The photolines arising from Cu 2p cores levels were, in general, weak indicating that the molecules are located inside the mesopores of MCM-41. CuPc (4%) supported on Ti-MCM-41 (Si/Ti = 40) showed a main peak at 934.1 eV and a shakeup (satellite) peak at around 946.0 eV corresponding to copper in +2 oxidation state. However, the main peak in the case of CuPc (4%) supported on Al-MCM-41 (Si/Al = 40) shifted to lower binding energy (932 eV) indicating that a part of copper on Al-MCM-41 is in a reduced +1 oxidation state [31]. This correlates well with the observations drawn from the EPR spectroscopy. The characterization studies, thereby, indicate that support and its acidic properties influence the support-metal complex interactions.

### 3.2 Catalytic Activity

Benzaldehyde was the selective product in the oxidation of benzyl alcohol with TBHP (70% aq.) over immobilized CuPc complexes (Table 2). The conversion of benzyl alcohol over different supports immobilized with 4 wt% of CuPc, decreased in the order: Al-MCM-41 > MCM-41 > Ti-MCM-41. It had increased with increasing amount of immobilized CuPc and substituted heteroatom (Al, for example). CuPc (4%) immobilized on Al-MCM-41 exhibited a conversion of 47.5% (Table 2). Controlled experiments revealed that the reaction occurs even in the absence of a catalyst but the conversion was low (17–26% in dioxane).

Solvent had a marked effect on the oxidation reaction (Fig. 5). The reaction was conducted in both polar and non-polar solvents. Reaction was also conducted without any solvent. While some solvents showed negative effect, highly polar solvents like dioxane, ethylacetoacetate (Et-acac) and dimethylsulfoxide (DMSO) showed promotional effects. Near quantitative conversion of benzyl alcohol to benzaldehyde was observed in DMSO and ethylacetoacetate. Highly polar solvents like DMSO facilitate formation of active oxygen species and thereby enhance the catalytic activity.

The molar ratio of TBHP to benzyl alcohol influenced the conversion as well as product selectivity (Fig. 6, left). The reaction was conducted in dioxane medium over Al-MCM-41(20)-CuPc(4). Although benzyl alcohol conversion had increased, the selectivity for benzaldehyde

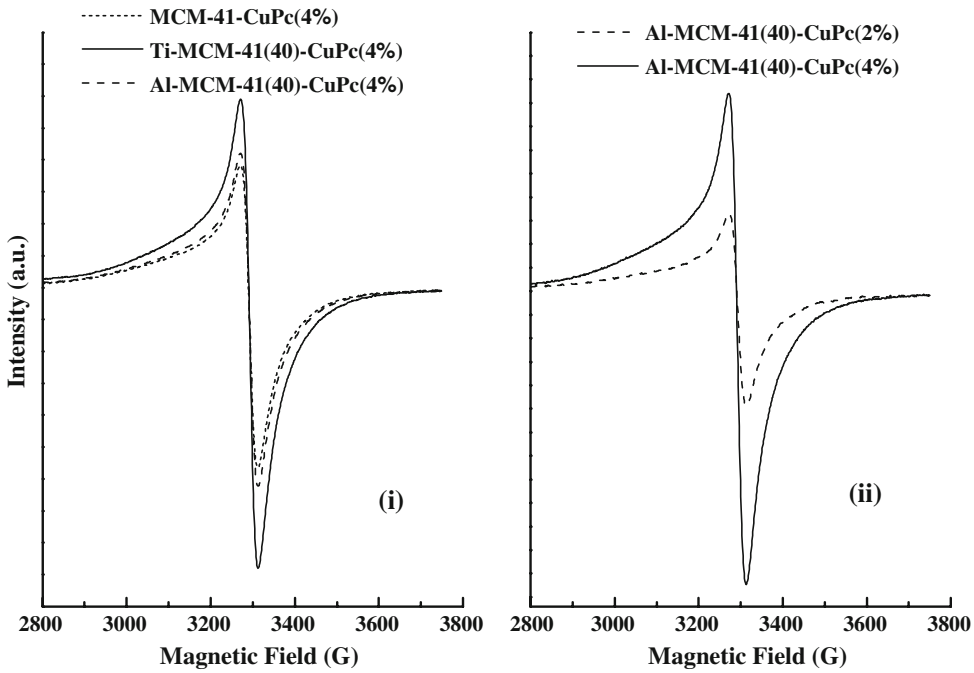


**Fig. 4** EPR spectra: (i) CuPc immobilized on different MCM-41 supports; (ii) Al-MCM-41 immobilized with different amounts of CuPc

**Table 2** Oxidation of benzyl alcohol over immobilized CuPc complexes

| Catalyst | Conversion (%) | Benzaldehyde selectivity (%) | Catalyst | Conversion (%) | Benzaldehyde selectivity (%) |
|---|---|---|---|---|---|
| Al-MCM-41(10) | 17.0 | 100 | Al-MCM-41(10)-CuPc(4) | 47.5 | 100 |
| Al-MCM-41(20) | 18.0 | 100 | Al-MCM-41(20)-CuPc(4) | 45.5 | 100 |
| Al-MCM-41(40) | 20.5 | 100 | Al-MCM-41(40)-CuPc(4) | 43.0 | 100 |
| | | | Al-MCM-41(40)-CuPc(2) | 31.0 | 100 |
| | | | Al-MCM-41(50)-CuPc(4) | 44.0 | 100 |
| Ti-MCM-41(20) | 26.5 | 100 | Ti-MCM-41(20)-CuPc(4) | 33.0 | 100 |
| Ti-MCM-41(40) | 24.5 | 100 | Ti-MCM-41(40)-CuPc(4) | 27.5 | 100 |
| | | | Ti-MCM-41(40)-CuPc(2) | 24.0 | 100 |
| MCM-41 | 18.5 | 100 | MCM-41-CuPc(4) | 36.0 | 100 |

Reaction conditions: Benzyl alcohol = 0.55 g, TBHP (70% aq.) = 0.98 g, benzyl alcohol/TBHP molar ratio = 1:1.5, catalyst = 0.055 g, solvent (dioxane) = 10 mL, reaction temperature = 373 K, reaction time = 4 h

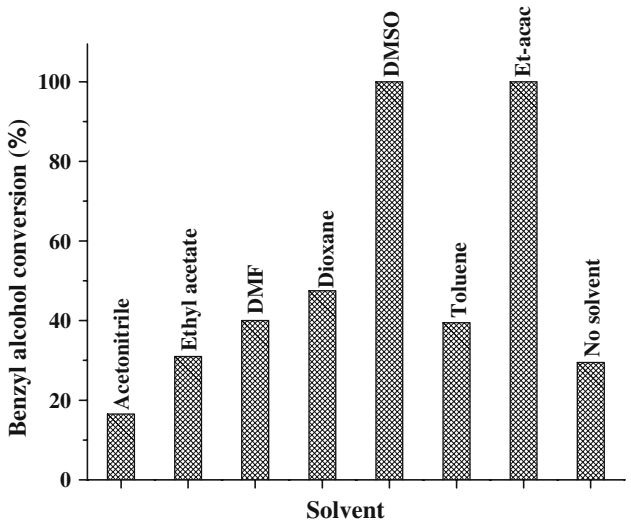


**Fig. 5** Influence of solvent on the oxidation of benzyl alcohol with TBHP over Al-MCM-41(10)-CuPc(4). Reaction conditions: Benzyl alcohol = 0.55 g, TBHP (70% aq.) = 0.98 g, benzyl alcohol/TBHP molar ratio = 1:1.5, catalyst = 0.055 g, solvent = 10 mL, reaction temperature = 373 K, reaction time = 4 h

decreased from 100 to 89% with increasing amounts of TBHP in the reaction. At higher concentrations of TBHP, benzaldehyde got further oxidized to benzoic acid. Hence, a molar ratio of 1.5 for TBHP to benzyl alcohol was found optimum.

Catalytic activity of Al-MCM-41(20)-CuPc(4) increased with increasing reaction temperature. However, above 373 K, the selectivity for benzaldehyde had decreased from 100 to 95.5% (Fig. 6, middle). The conversion of benzyl alcohol increased with increasing amount of catalyst up to 15 wt% (Fig. 6, right). It may be noted that the amount of the catalyst did not influence the product selectivity.

Conversion of benzyl alcohol increased with increasing reaction time, reached a maximum at around 4 h and beyond that the increase was only marginal. The data could be fitted to first-order kinetics. Activation of TBHP and formation of reactive oxygen species (ROS) are, possibly, the rate-determining steps. The ROS abstract the benzylic proton and oxidize benzyl alcohol to benzaldehyde. The rate constants for this reaction were found to be $17.04 \times 10^{-4}$,

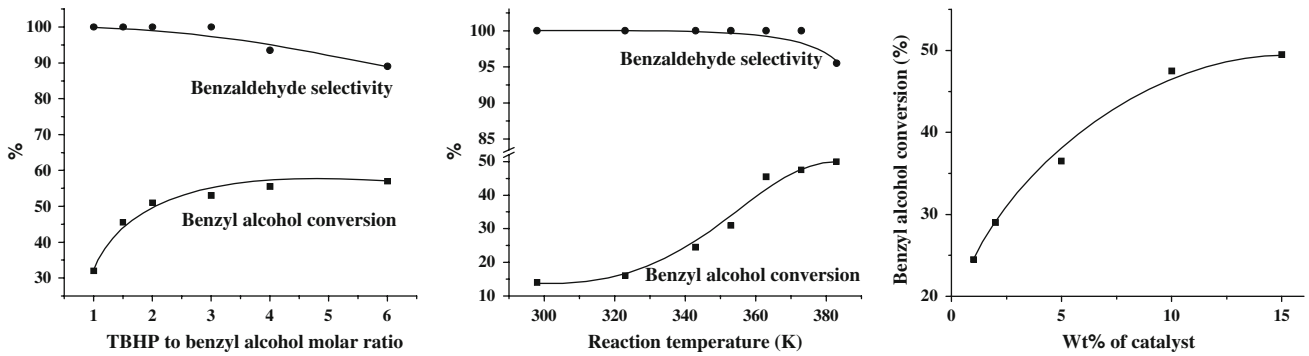


**Fig. 6** Oxidation of benzyl alcohol with TBHP over Al-MCM-41(20)-CuPc(4). *Left* effect of oxidant to substrate molar ratio. Reaction conditions: benzyl alcohol = 0.55 g, catalyst = 0.055 g, oxidant = TBHP (70% aq.), dioxane (solvent) = 10 mL, reaction temperature = 373 K, reaction time = 4 h. *Middle* effect of temperature. Reaction conditions: same as above except TBHP (70% aq.) = 0.98 g. *Right* effect of amount of catalyst. Reaction conditions: same as above except reaction temperature = 373 K

$17.73 \times 10^{-4}$, $19.34 \times 10^{-4}$, and $22.34 \times 10^{-4}$ $s^{-1}$ at 353, 363, 368, and 373 K, respectively. The activation energy was estimated to be 14.8 kJ $mol^{-1}$. The reaction occurred even when molecular oxygen instead of TBHP was used as oxidant. A conversion of 45% was obtained over Al-MCM-41(20)-CuPc(4). But the selectivity for benzaldehyde was only 90% (instead of 100% that was obtained with TBHP oxidant).

Reusability of the catalyst was confirmed in three recycling experiments. At the end of each run the catalyst was separated, washed with dioxane and acetone and dried at 373 K for 3 h. It was then used in the subsequent oxidation reactions. The selectivity for benzaldehyde (100%) was unaffected. However, the catalytic activity (benzyl alcohol conversion) decreased marginally from 43 to 40% at the end of third recycle over Al-MCM-41(40)-CuPc(4) catalyst. It was confirmed by elemental composition that this marginal decrease in catalytic activity was not due to leaching of metal ions or destruction of CuPc complex but due to adsorption of product molecules.

EPR signal intensity revealed that the acidity of the support influences the oxidation state of Cu in CuPc. A part of copper is reduced from +2 to +1 "formal" oxidation state when supported on Brönstend acidic Al-MCM-41. Such a reduction of $Cu^{2+}$ ions was more pronounced when CuPc was supported on Al-MCM-41 than on pure siliceous MCM-41 and Ti-MCM-41. Catalytic activity parallels the variation in $Cu^{1+}$ concentration in different catalyst samples (Fig. 7). This indicates that copper in a reduced form is, possibly, the active site. Such reduced forms of copper are more available on Al-MCM-41 and hence, higher catalytic activity was observed for CuPc supported on Al-MCM-41. In fact, copper ions with an oxidation state of +1 have been invoked in the mechanism of benzyl alcohol oxidation to benzaldehyde over galactose oxidase [20, 21]. The present study, thus, reveals that by suitably modifying the acidic properties of the support one can fine-tune and modulate the electronic and catalytic properties of the active oxidation sites.

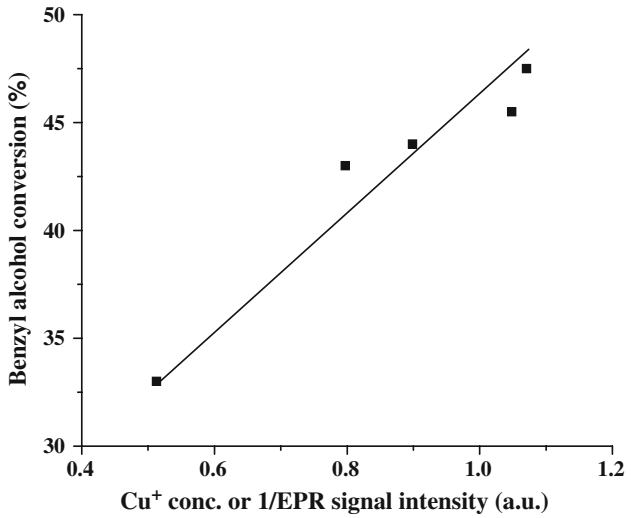


**Fig. 7** Correlation between $Cu^{+}$ ion concentration and catalytic activity of immobilized CuPc complexes

## 4 Conclusions

Copper phthalocyanine (CuPc) complexes immobilized on MCM-41, Ti-MCM-41, and Al-MCM-41 exhibit high catalytic activity in the oxidation of benzyl alcohol to selectively benzaldehyde with peroxides and molecular oxygen as oxidant. The acidity of the support influenced the electronic structure (oxidation state) of copper in CuPc. A part of copper was reduced from +2 to +1 oxidation state when supported on Brönsted acidic Al-MCM-41. A direct relation between $Cu^{+1}$ concentration and catalytic oxidation activity was observed. The study demonstrates the important role of support on the catalytic activity of immobilized CuPc complexes as like in metalloenzymes where the protein mantle influences the structure and the activity of active metal sites.

## References

1. Sheldon RA, Arends AI, Hanefeld U (2007) Green chemistry and catalysis. Wiely-VCH Verlag GmbH & Co KgaA, Weinheim
2. Ullmann F (2003) Ullmann's encyclopedia of industrial chemistry. Wiley-VCH Verlag, Weinheim
3. Kroschwitz JI (1992) Kirth Othmer encyclopedia of chemical technology, vol 4, 4th edn. Wiley-Interscience, New Delhi
4. Cainelli G, Cardillo G (1984) Chromium oxidations in organic chemistry. Springer, Berlin
5. Lee DG, Spitzer UA (1970) J Org Chem 35:3589
6. Menger FM, Lee C (1981) Tetrahedron Lett 22:1655
7. Mallat TM, Baiker A (1994) Catal Today 19:247
8. Kluytmans JHJ, Markusse AP, Kuster BFM, Marin GB, Schouten JC (2000) Catal Today 57:143
9. Besson M, Gallezot P (2000) Catal Today 57:127
10. Ferri D, Mondelli C, Krumeich F, Baiker A (2006) J Phys Chem B 110:22982
11. Grunwaldt JD, Caravati M, Baiker A (2006) J Phys Chem B 110:25586
12. Sawayama Y, Shibahara H, Ichihashi Y, Nishiyama S, Tsuruya S (2006) Ind Eng Chem Res 45:8837
13. Dimitratos N, Lopez-Sanchez JA, Morgan D, Carley A, Prati L, Hutchings GH (2007) Catal Today 122:317
14. Choudhary VR, Jha R, Jana P (2007) Green Chem 9:267
15. van Bekkum H (1991) In: Lichtenthaler FW (ed) Carbohydrates as organic raw materials, VCH, Weinheim
16. Choudhary VR, Dumbre DK, Uphade BS, Narkhede VS (2004) J Mol Catal A: Chem 215:129
17. Mohan Reddy K, Balaraju M, Sai Prasad PS, Suryanarayana I, Lingaiah N (2007) Catal Lett 119:304

18. Opre Z, Ferri D, Krumeich F, Mallat T, Baiker A (2006) J Catal 241:287
19. Kumar D, Bhat RP, Samant SD, Gupta NM (2005) Catal Commun 6:627
20. Klinman JP (1996) Chem Rev 96:2541
21. Solomon EI, Baldwin MJ, Lowery MD (1992) Chem Rev 92:521
22. Srinivas D, Sivasanker S (2003) Catal Surv Asia 7:121
23. Ratnasamy P, Raja R, Srinivas D (2005) Philos Trans A: Math, Phys and Eng Sci 363:1001
24. Deshpande S, Srinivas D, Ratnasamy P (1999) J Catal 188:261
25. Seelan S, Sinha AK, Srinivas D, Sivasanker S (2000) J Mol Catal A: Chem 157:163
26. Beck JS, Vartuli JC, Roth WJ, Leonowicz ME, Kresge CT, Schmitt KD, Chu CT W, Olson DH, Sheppard EW, McCullen SB, Higgins JB, Schlenker JL (1992) J Am Chem Soc 114:10834
27. Kresge CT, Leonowicz ME, Roth WJ, Vartuli JC, Beck JS (1992) Nature 359:710
28. Satyarthi JK, Saikia L, Srinivas D, Ratnasamy P (2007) Appl Catal A: Gen 330:145
29. Chaudhari K, Bal R, Srinivas D, Chandwadkar AJ, Sivasanker S (2001) Micropor Mesopor Mater 50:208
30. Joseph T, Srinivas D, Gopinath CS, Halligudi SB (2002) Catal Lett 83:209
31. Wan Y, Ma J, Wang Z, Zhou W, Kaliaguine S (2005) Appl Catal B: Enzym 59:235